

# Altered DNA repair creates novel Alu/Alu repeat-mediated deletions

Maria E. Morales<sup>1</sup> | Tiffany Kaul<sup>1</sup> | JaNiece Walker<sup>2</sup> | Chelsea Everett<sup>1</sup> |  
Travis White<sup>1,3</sup> | Prescott Deininger<sup>1,4</sup> 

<sup>1</sup>Tulane Cancer Center, Tulane University, New Orleans, Louisiana, USA

<sup>2</sup>Department of Biology, Xavier University, New Orleans, Louisiana, USA

<sup>3</sup>Memorial Sloan Kettering Cancer Center, New York, New York, USA

<sup>4</sup>Department of Epidemiology, Tulane University, New Orleans, Louisiana, USA

## Correspondence

Prescott Deininger, Tulane Cancer Center, Tulane University, New Orleans, LA 70112, USA.

Email: [pdeinin@tulane.edu](mailto:pdeinin@tulane.edu)

## Funding information

National Institute of General Medical Sciences, Grant/Award Numbers: R01 GM121812, R15 GM118966

## Abstract

Alu elements are the most abundant source of nonallelic homology that influences genetic instability in the human genome. When there is a DNA double-stranded break, the Alu element's high copy number, moderate length and distance and mismatch between elements uniquely influence recombination processes. We utilize a reporter-gene assay to show the complex influence of Alu mismatches on Alu-related repeat-mediated deletions (RMDs). The Alu/Alu heteroduplex intermediate can result in a nonallelic homologous recombination (HR). Alternatively, the heteroduplex can result in various DNA breaks around the Alu elements caused by competing nucleases. These breaks can undergo Alt-nonhomologous end joining to cause deletions focused around the Alu elements. Formation of these heteroduplex intermediates is largely RAD52 dependent. Cells with low ERCC1 levels utilize more of these alternatives resolutions, while cells with *MSH2* defects tend to have more RMDs with a specific increase in the HR events. Therefore, Alu elements are expected to create different forms of deletions in various cancers depending on a number of these DNA repair defects.

## KEYWORDS

Alu elements, DNA double-stranded break repair, heteroduplex rejection, homologous recombination, repeat-mediated deletions

## 1 | INTRODUCTION

Repetitive elements comprise at least 45% the human genome (Lander et al., 2001) and cause repeat-mediated deletions (RMDs) through recombination between nonallelic copies (Deininger & Batzer, 1999; Gu et al., 2015; Mendez-Dorantes et al., 2018; Sen et al., 2006). The high abundance of Alu elements in the human genome creates a major source of these nonallelic homologies, which influence DNA double-strand break (DSBs) repair and lead to altered forms of genetic instability mediated by Alu-related RMDs

(Callinan et al., 2005; Cordaux & Batzer, 2009; Hedges et al., 2004). With over 1 million copies in the human genome (about 11% of the overall mass of DNA), Alu elements are distributed across all chromosomes, though they tend to cluster in gene-rich regions (Lander et al., 2001). This means that Alu element-related instability frequently results in genomic rearrangements that influence gene function (Kaul et al., 2017; Sen et al., 2006; Xing et al., 2007). Alu-related RMDs in germ cells have been linked to many diseases, including Parkinson's disease, several cancers, and pulmonary artery hypertension (Morales et al., 2015). These events primarily occur relatively locally within a

This is an open access article under the terms of the Creative Commons Attribution-NonCommercial-NoDerivs License, which permits use and distribution in any medium, provided the original work is properly cited, the use is non-commercial and no modifications or adaptations are made.

© 2021 The Authors. *Human Mutation* published by Wiley Periodicals LLC

chromosome (Belancio et al., 2010; Pavlicek et al., 2004) resulting in deletion or duplication of exons in a gene, but they also can occur over larger distances, causing more complex chromosomal abnormalities (Hu et al., 2019; Mendez-Dorantes et al., 2018).

The primary factor leading to Alu-related RMDs in the human genome is the occurrence of a DSB near these repetitive sequences (White et al., 2015). In eukaryotic cells, two broad types of pathways are known to efficiently repair DNA DSBs: nonhomologous end joining (NHEJ) and homologous recombination (HR) (Kass & Jasin, 2010; Symington & Gautier, 2011). Homology-based repair generally requires resection of one DNA strand to expose single strand(s) at the DSB (Figure 1a). This is followed by either (1) intrachromosomal

annealing of repetitive sequences in exposed single strands on both sides of the DSB (Figure 1b) or (2) an invasion into a nearby duplex region with HR or break induced replication (BIR) (Figure 1d) (Bhargava et al., 2016). Either of these nonallelic interactions is likely to lead to an intermediate with two key elements; a 3' flap and a 300 bp heteroduplex (Figures 1b and 1d). ERCC1/XPF endonuclease has a suggested role in the repair of DNA DSB with single-strand annealing (SSA) by cleaving the 3' flaps and filling in the gaps (Figures 1c and 1e) (Al-Minawi et al., 2008).

In addition to their repetitive nature, the mismatches between Alu elements also increase the complexity of their interaction with DNA repair processes. We have previously shown that nonallelic,

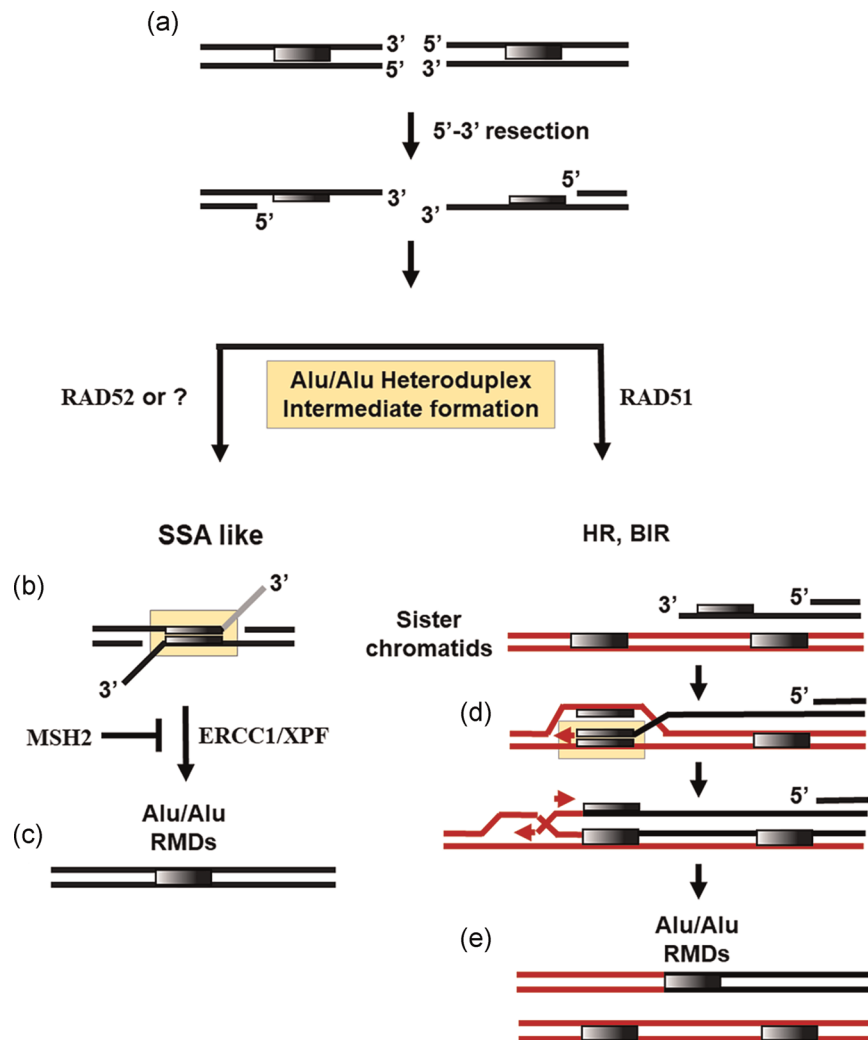


**FIGURE 1** Double-strand break repair between Alu elements. (a) After a double stranded break (DSB) in DNA, 5'-3' resection can occur. It results in single-stranded DNA that provides a platform for recruitment of repair proteins that participate in homology directed DSB repair. (b) Based on the single strand annealing (SSA)-like model, after end resections, repeats come together to form a heteroduplex intermediate. One of the main proteins involved in this pathway is RAD52. This intermediate is prone to disassociation by heteroduplex rejection, which is mediated by proteins including MSH2. (c) Processing by ERCC1/XPF and repair can result in an Alu/Alu repeat mediated deletions (RMDs). (d) End resections may also be resolved with homologous recombination (HR) or break induced replication (BIR) DNA repair pathways that involve RAD51. The single-stranded DNA repeat can invade the other repeat in the sister chromatid to create an Alu/Alu heteroduplex. This could give rise to an identical deletion product seen in the SSA-like repair pathway at the level of analysis in our assay

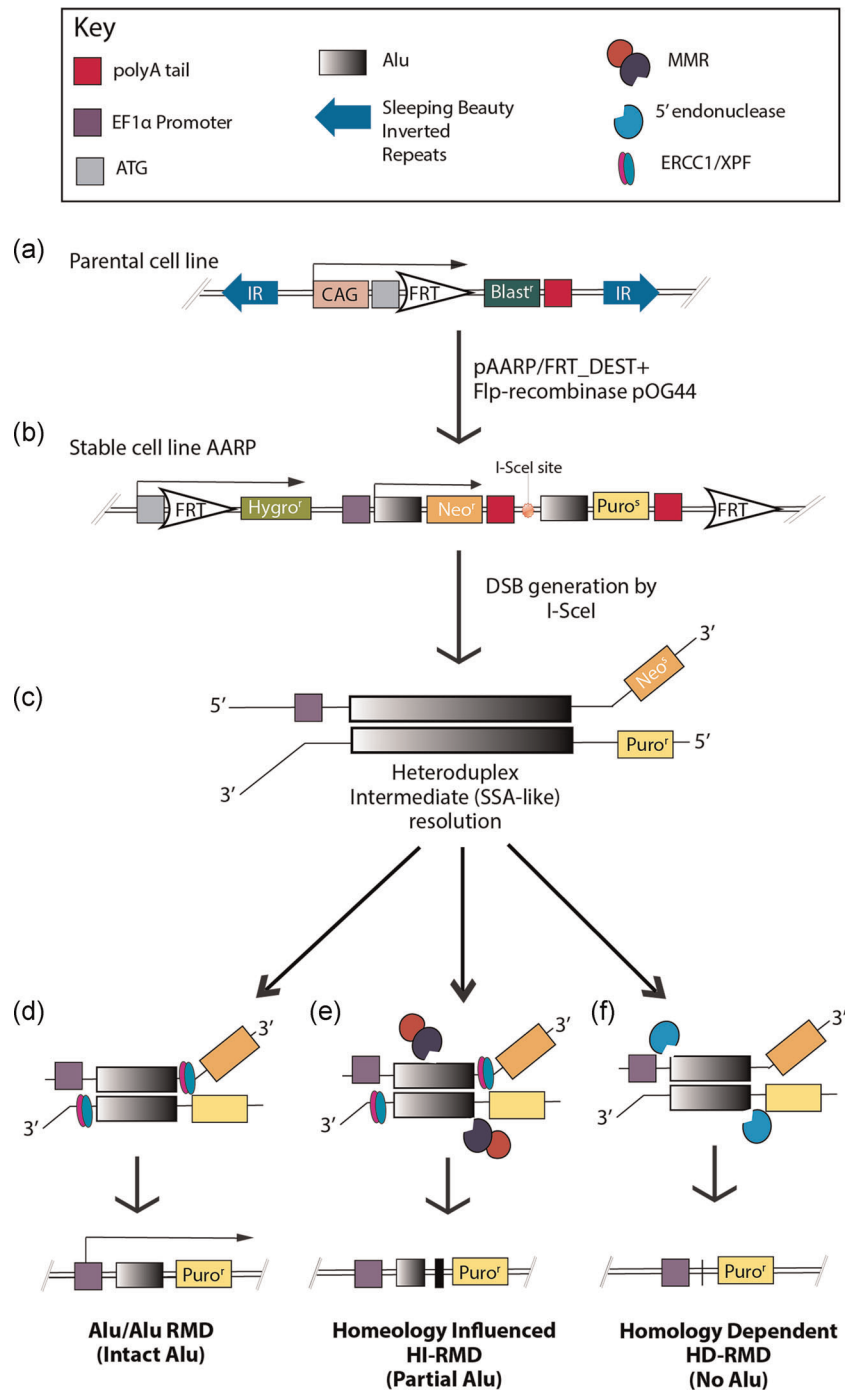


**FIGURE 2** (a) Schematic of sleeping beauty FRT Flp-In target site in HeLa parental cell lines. Cells with the integrated sleeping beauty FRT Blast were blasticidin resistance (Blast<sup>r</sup>). (b) AARP stable cell lines were created by site specific recombination at the FRT site. The AARP reporter cassette contains the hygromycin-resistance (Hygro<sup>r</sup>) gene used to select a stable cell line upon Flp-recombinase-mediated integration of the cassette. The AARP reporter cassette contains a human elongation factor 1 $\alpha$  (EF1 $\alpha$ ) promoter upstream of the neomycin resistance (Neo<sup>r</sup>) gene. An I-Sce1 endonuclease cleavage site is positioned between the two Alu elements that are spaced apart by 1.1 kb. Before DNA repair, the puromycin resistance (puro<sup>r</sup>) gene was not expressed due to distance from the EF1 $\alpha$  promoter and interruption by the Neo<sup>r</sup> gene and polyadenylation (pA) site, which results in puromycin sensitivity (puro<sup>s</sup>). (c) Repair of an I-Sce1-induced DSB may result in a SSA-like deletion of the sequence between the two Alu elements after which the cells become neomycin sensitive and expressed the puro<sup>r</sup> gene. (d) Alu/Alu RMD gives rise to a breakpoint junction containing an intact Alu. This is mediated by a 3' flap (ERCC1/XPF endonuclease). (e) Homeology Induced events (HI-RMD) in the form of alt-NHEJ causes new DNA cleavage in the heteroduplexed Alu elements and alt-NHEJ of these new ends gives rise to a breakpoint junction with partial Alus. This is mediated by mismatch repair (MMR) and ERCC1/XPF. (f) Another variation of Alt-NHEJ, homology dependent-RMD (HD-RMD), gives rise to a breakpoint junction with no Alu. This is mediated by a 5' flap endonuclease. DSB, double-strand break; NHEJ, nonhomologous end joining; SSA, single-strand annealing

RMDs relying on HR, referred to as Alu/Alu-related RMDs, occur at the highest rate when there is no sequence divergence (Figure 2d) (Morales, White, et al., 2015). As sequence divergence increases, a homeology-modified form of alt-NHEJ, referred to as homeology-induced RMDs (HI-RMDs) involving the DNA mismatch repair (MMR) pathway becomes more predominant (Figure 2e) (Morales et al., 2015). In this study we introduce a novel DNA repair pathway referred to as homology-dependent RMDs (HD-RMDs) (Figure 2f) that occur with increased sequence homology. These findings demonstrate that sequence divergence between the involved Alu elements may be a critical factor influencing the choice between several competing DNA repair processes.

We are only beginning to understand the complexity of the DNA repair processes influenced by Alu homeologies. Here we have used our Alu-related RMD system (Morales et al., 2015) to evaluate the relative use of different Alu/Alu interaction pathways in the tumor cell lines, HeLa and HEK293, to identify involved DNA repair genes. We show for the first time that HeLa cells expressing low levels of ERCC1 generate a unique HD-RMD breakpoint junction that eliminates both interacting Alu elements. In addition, cells deficient in MMR with *MSH2* knockout (KO) show a significant increase on Alu-related RMD rates and shift their repair from HI-RMD to Alu/Alu RMDs. Strikingly, cells deficient in *RAD52* had a decreased RMD rate in homologous repeats and an increase in RMD rate in divergent Alu/Alu RMDs. *RAD52* KO cells also had a shift in their repair from Alu/Alu RMDs with an intact Alu to HI-RMDs with a partial Alu. In conjunction, these results show a strong link between deficiencies in MMR and chromosomal instability associated with Alu-related RMDs.

## 2 | MATERIALS AND METHODS

### 2.1 | FRT cells and cell culture

We obtained HeLa cells from American Type Culture Collection and Flp-In<sup>TM</sup>-293 cells with an FRT site from Thermo Fisher Scientific. HeLa-FRT cells were generated using the Sleeping Beauty cassette as previously described in (Mátés et al., 2009) HeLa-FRT cells were maintained in minimum essential medium (MEM) with 10% fetal bovine serum (FBS; Gibco, Invitrogen), nonessential amino acids and sodium pyruvate (Invitrogen). HEK293-FRT cells were maintained in DMEM with 10% FBS (Invitrogen).

Briefly, to generate the HeLa-FRT cell lines, one million HeLa cells were seeded per 75 cm<sup>2</sup> flask. One day after seeding, cells were cotransfected with pT2/FRT-Blast transposon donor plasmid and the second plasmid coding for SB100X transposase (Mátés et al., 2009) using Lipofectamine and Plus (Invitrogen) according to the manufacturer's protocol. In our protocol, the amount of both pT2/FRT-Blast and transposase coding plasmids were 25 ng for HeLa cell lines. All the transfection reactions were filled up to 1000 ng total DNA using a filler pUC19 plasmid. The plasmids, upon integration by transposition, yielded cells resistant to the

antibiotic Blasticidin, allowing measurement of transposition. Forty-eight hours after transfection, media containing Blast was added to select for integration events. Blast selection was maintained for 14 days until visible colony formation. All cells were cultured at 37°C in a humidified 5% CO<sub>2</sub> atmosphere.

### 2.2 | Generation of stable Alu/Alu recombination puro (AARP) cell lines

To develop stable Alu/Alu recombination cell lines, all destination vectors using 0%, 5%, and 15% Alu sequence divergence were integrated into the FRT site of each parental cell line. Specifically, we flipped in 100 ng of each destination vector (0%, 5%, and 15%) with 900 ng of the flippase recombinase expression plasmid pOG44 using Lipofectamine and Plus reagent according to manufacturer's protocol (Thermo Fisher Scientific) (Figure 2a,b). For these experiments,  $1.0 \times 10^6$  cells for HEK293-FRT and HeLa-FRT were seeded in a T75 culture flask 24 h before transfection. Forty-eight hours after transfection, medium was replaced with fresh medium containing 75 µg/ml of hygromycin for HEK293-FRT cells and 150 µg/ml of hygromycin for HeLa-FRT cells. The medium was changed every 3 days. Twelve days after hygromycin selection, three independent clones were selected for Alu-related RMD analysis. Individual hygromycin resistant clones were expanded and maintained in medium containing 500 µg/ml neomycin (Thermo Fisher Scientific). As a negative control, all Alu/Alu recombination destination vectors were transfected without the pOG44 recombinase vector and no hygromycin resistant clones were detected.

### 2.3 | AARP recombination assays

The 0%, 5%, and 15% AARP HeLa and HEK293 cell lines were grown in 400 µg/ml G418-MEM + 10% FBS + nonessential amino acids and sodium pyruvate (Invitrogen) and 600 µg/ml G418-DMEM + 10% FBS to select against background recombination events, respectively. The different clonal AARP HEK293 and HeLa cell lines were seeded in T-75 flasks at a density of  $1 \times 10^5$  cells/flask. For an exogenous source of DSBs, cells were transfected 16–24-h postseeding with 1.0 µg of *I-SceI* expression plasmid pSCBase (Morales et al., 2015), using Lipofectamine and PLUS Reagents according to manufacturer's protocol (Thermo Fisher Scientific). After 5 h, the transfection medium was replaced by complete medium. After 48 h, the cells were grown for 2 weeks using Puromycin selection medium (containing 1.0 µg/ml puromycin for HeLa and 1.3 µg/ml for HEK293) to obtain resistant (puro<sup>r</sup>) colonies. Cell colonies were fixed and stained for 30 min with crystal violet solution (0.2% crystal violet in 5% acetic acid and 2.5% isopropanol). Colonies were counted using a ColCount automated colony counter from Oxford Optronix. Each

transfection was performed a minimum of three times in parallel using independent clones in duplicates for each construct and cell type. An additional transfection was performed in parallel to isolate genomic DNA from colonies that were grown to analyze the DNA repair events by PCR and sequencing. A schematic of the AARP construct and the recombination assay is shown in Figure 2.

## 2.4 | Analysis of DNA repair events

Genomic DNA from isolated puro<sup>r</sup> clones was extracted using the DNeasy Blood and Tissue kit (Qiagen). A total of 200–500 ng of genomic DNA was PCR amplified in a 50  $\mu$ l GoTaq (Promega) reaction as per manufacturer recommendations with the addition of 5% dimethyl sulfoxide. Primers designed to amplify the sequence located between the EF1 $\alpha$  promoter and the puro<sup>r</sup> gene were the following: EF1 5'-GAGAATCGGACGGGGGTAGT-3' and RP1 5'-GCTCGTAGAAGGGCAGGTTG-3'. PCR amplification with these primers make, a product of 1508 bp with DNA repair through Alu/Alu RMD with a resulting intact Alu. A variety of smaller sized products result in cells that have undergone HI-RMDs and HD-RMDs. PCR products were cloned into the TOPO TA vector (TOPO TA Cloning Kit; Thermo Fisher Scientific) and sequenced by chain termination (Elim Biopharmaceuticals) using AARP sequencing primer previously described in Morales et al. (2015; Sanger et al., 1997).

## 2.5 | Generation of ERCC1, MSH2, and RAD52 KO cells with CRISPR/Cas9-eGFP and flow cytometry

KO of ERCC1, MSH2, and RAD52 was performed by transiently transfecting with CRISPR/Cas9 KO plasmids (Cat# sc-400630, Cat# sc-400966, Cat# sc-401948, respectively; Santa Cruz Biotechnology). ERCC1, MSH2, and RAD52 KO plasmids were obtained from Santa Cruz Biotechnology. In brief,  $1 \times 10^6$  (HeLa and HEK293) cells were seeded at 24 h before transfection in T75 flasks. Cells were transfected with 2.0  $\mu$ g of CRISPR/Cas9 KO plasmid using Lipofectamine and Plus (Thermo Fisher Scientific). After 48-h posttransfection, eGFP-positive cells were selected by fluorescence-activated cell sorting (FACS) using FACS Aria (BD Biosciences). Single-cells were seeded in 96-well plates by FACS and expanded. KO cells were confirmed by immunoblotting analysis.

## 2.6 | ERCC1, MSH2, RAD52 transient complementation in cells

HEK293 and HeLa cells were seeded at  $1.5 \times 10^5$  cells per T75 flask and transfected 16–18 h later with 1.0  $\mu$ g of the human ERCC1, MSH2, or RAD52 expression vector.

Transfections with the empty vector, pCCAG, were used as controls (Servant et al., 2017). After 5 h, serum-free media was

replaced with serum-containing media, and the cells were harvested at 48 h after transfection for western blot. For colony assays and the rescue of DSB breakpoint junctions, cells were grown for 2 weeks using puromycin selection medium (containing 1.0  $\mu$ g/ml puromycin) to obtain puro<sup>r</sup> colonies.

## 2.7 | Immunoblotting analysis of the KO cells and complementation vectors

Protein was extracted from cell lysates using tissue lysis buffer-SDS buffer (0.5% (wt/vol) SDS, 0.5% (vol/vol) Triton X-100, 150 mM NaCl, 10 mM ethylenediaminetetraacetic acid, 50 mM Tris pH 7.2). Protein was separated on a 4%–12% Tris-Glycine gel (Thermo Fisher Scientific) and blotted using a mouse monoclonal antibody specific to ERCC1, MSH2, and RAD52 (Santa Cruz Biotechnology). ERCC1, MSH2, and RAD52 detection was done using a goat anti-mouse horseradish peroxidase conjugated antibody (Santa Cruz Biotechnology) and visualized and quantified on a ChemiDoc (BioRad).

## 2.8 | Statistical analysis

For comparing means of two groups, statistical evaluation was performed with two-tailed, Student's *t* tests using GraphPadPrism 8 software. *SE* of the mean (*SEM*) of at least three independent experiments was calculated to understand variability. For comparing observed versus expected categorical groups, significance was calculated using the  $\chi^2$  tests. The *p* values were considered significant if *p* < .05.

# 3 | RESULTS

## 3.1 | Integration of the AARP system and its different types of breakpoint junctions

We have developed an Alu/Alu recombination reporter system that integrates Alu variants into a recombination cassette into a unique FRT site in the genome using FRT recombinase (Figure 2a) (Morales, Servant, et al., 2015). This allows us to assess alterations in recombination rate within a consistent chromatin environment. To generate stable parental cell lines with a single FRT site, we used a *Sleeping beauty* transposon-based system carrying a FRT site (Figure 2a) (Mátés et al., 2009). We then introduced our AARP cassette into the FRT site following the protocol listed in Morales et al. (2015). We stably integrated AARP into the genome of HeLa FRT cells and isolated individual hygromycin- and neomycin-resistant clones (Figure 2b). Three independent FRT-integrated cell clones for each AARP variant were selected and transiently transfected with an I-Sce1 endonuclease expression vector to induce formation of DNA DSBs

between the two Alu elements (Figure 2c). Recombination was determined by the transition from neomycin to puromycin resistance (Figure 2d-f) that allows for a colony-based assay.

One key feature of our AARP cassette is that it allows for the selection of a variety of deletion junctions involving the sequence in the vicinity of the two Alu elements. This occurs because the junctions are not within coding regions, which permits imprecise junctions. Any deletion of the neomycin resistance gene and polyadenylation signal brings the Puro<sup>R</sup> gene into proximity of the EF1 $\alpha$  promoter to confer Puro<sup>r</sup> (Figure 2c-f). We have shown that the AARP recombination system was able to resolve a targeted DSB between the Alu elements using different DNA repair processes: (1) An Alu/Alu RMD, which gives rise to a breakpoint junction containing an intact Alu (Figure 2d), (2) homeology induced event in the form of alt-NHEJ (HI-RMD) which causes deletions in the vicinity of the two Alu elements and gives rise to a breakpoint junction with partial Alus (Figure 2e), and (3) Another variation of Alt-NHEJ, homology dependent-NHEJ (HD-RMD), which gives rise to a breakpoint junction with no Alu (Figure 2f).

### 3.2 | HeLa cells have decreased Alu-related RMD rates and give rise to a unique type of breakpoint junction

We have previously characterized Alu-related instability with our reporter system in HEK293 and HCT116 cells and observed differences in the types of resolution of mismatched Alu elements (Morales et al., 2015). We chose to look further at HeLa cells as another example of a cancer cell likely to exhibit altered DNA repair properties. The 0%, 5%, and 15%-mismatch AARP cassettes containing Alu sequences were integrated in the HeLa FRT cells. Figure 3a,b show that 0%, 5%, and 15%-AARP HeLa cells repair the I-Sce1-generated DSB resulting in puromycin-resistant colonies in a pattern similar to HEK293 cells (Morales et al., 2015). As expected, we observed a significant drop in Alu-related RMD rate in 5% AARP relative to the homologous Alu elements with 0% AARP (Figure 3a). Further, the 15% AARP construct showed a significant increase in Alu-related RMDs when compared to the 5% AARP (Figure 3a). This significant increase is the result of a shift in DSB DNA repair pathways from homology-dependent mechanisms to Alt-NHEJ (Figure 3c,d). Repair via NHEJ was

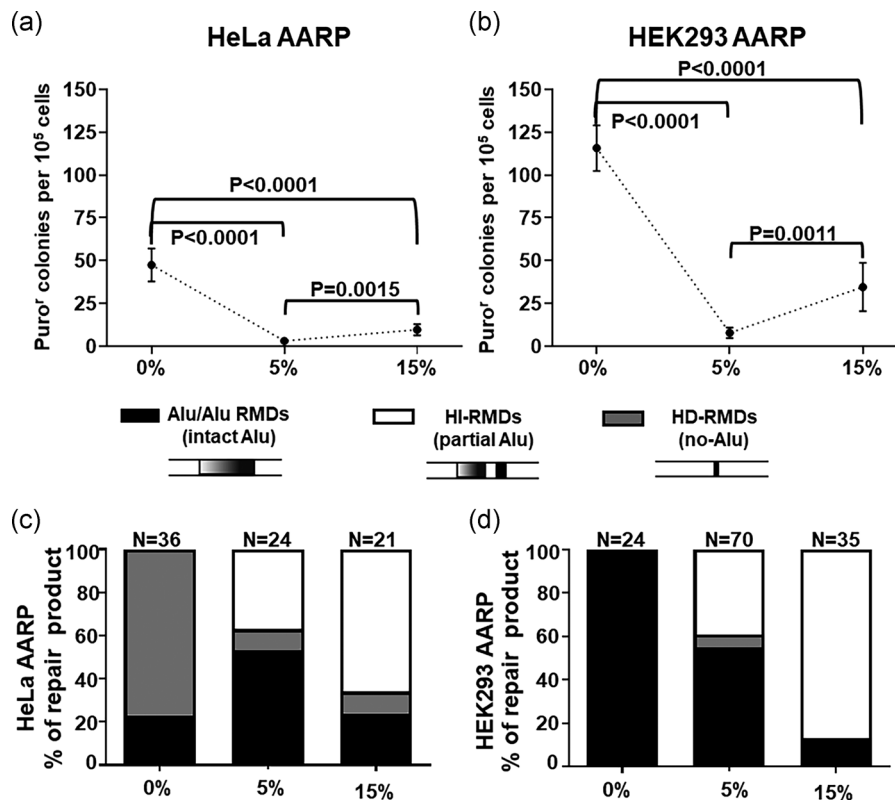


**FIGURE 3** (a) The average number of puromycin-resistant colonies is plotted for AARP HeLa cells. Data from at least three independent experiments using at least three independently isolated clones for each AARP cell line are averaged. Error bars denote standard error and statistical significance is shown using student *t* test. (b) The average number of puromycin-resistant colonies is plotted for the indicated AARP HEK293 cells. Data from at least three independent experiments using at least three independently isolated clones for each AARP cell line are averaged. Error bars denote standard error and statistical significance is shown using student *t* test. (c, d) Depicted are the percentages of Alu/Alu RMDs (in black), HD-NHEJ (in gray), and HI-NHEJ (in white) as determined by sequence analysis of DNA repair products from isolated puromycin-resistant colonies. AARP, Alu/Alu recombination puromycin; NHEJ, nonhomologous end joining; RMD, repeat-mediated deletion

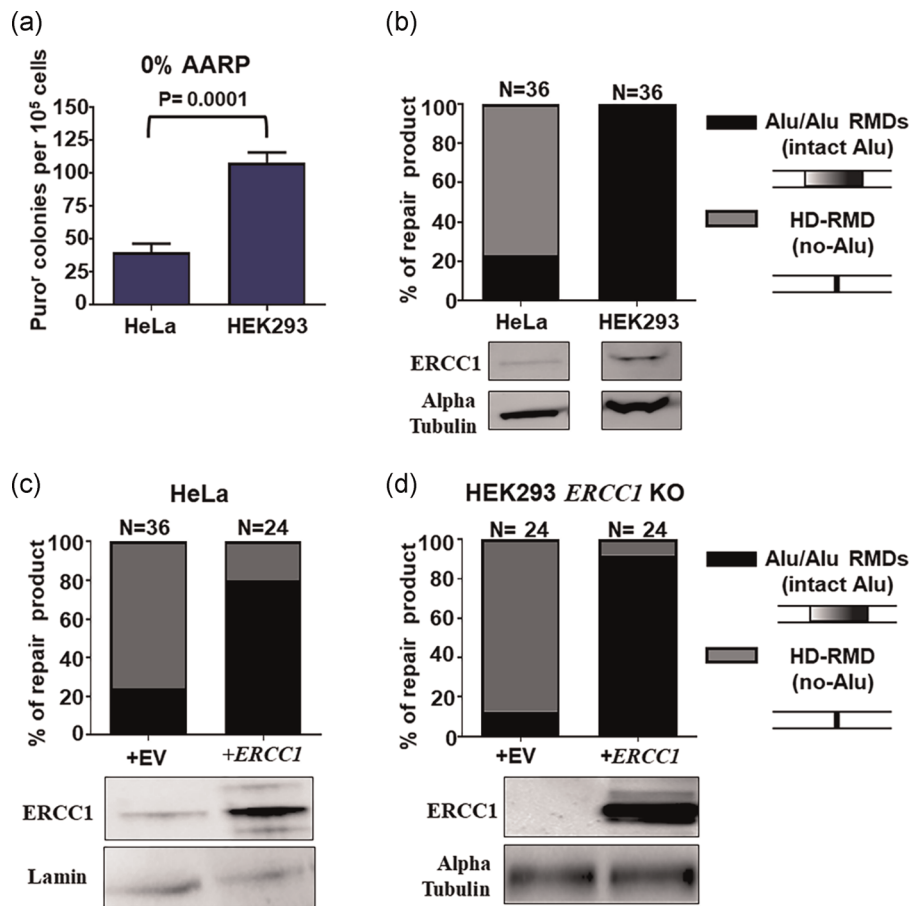


**FIGURE 4** (a) The average number of puro<sup>+</sup> colonies is plotted for 0% AARP HeLa and HEK293 cells. Data from at least three independent experiments using at least three independently isolated clones for each AARP cell line are averaged. Error bars denote SE and statistical significance is shown using student *t* test. (b) The percentage of Alu/Alu RMDs and HD-RMDs as determined by sequence analysis of DNA repair products from isolated puro<sup>+</sup> colonies in HeLa and HEK293 WT cells. The western blots of ERCC1 levels are shown in HeLa and HEK293 cells. These bands come from a single Western blot probed separately with the appropriate antibodies and only the relevant lanes from that blot are presented. (c) The percentage of Alu/Alu RMDs and HD-RMDs as determined by sequence analysis of DNA repair products from isolated puro<sup>+</sup> colonies in HeLa WT+EV and HeLa WT +ERCC1 cells. Western blots of ERCC1 levels are shown in HeLa WT +EV and HeLa WT +ERCC1 cells. (d) The percentage of Alu/Alu RMDs and HD-RMDs as determined by sequence analysis of DNA repair products from isolated puro<sup>+</sup> colonies in HEK293 ERCC1 KO +EV and HEK293 ERCC1 KO +ERCC1 cells. The western blots of ERCC1 levels are shown in HEK293 ERCC1 KO +EV and HEK293 ERCC1 KO +ERCC1 cells. AARP, Alu/Alu recombination puro; KO, knockout; RMD, repeat-mediated deletion

responsible for the vast majority of products that involve two Alu elements with 15% sequence divergence in HeLa cells (Figure S1). Interestingly, when the Alu elements both match one another perfectly (0% mismatch), there appear to be fewer colonies than with HEK293 cells (Figures 3a,b, and 4a). More surprisingly, sequence analysis of the HeLa repair junctions did not represent the typical intact Alu/Alu RMD products seen in HEK293 cells (Morales et al., 2015), but instead represented relatively precise deletion of both Alu elements and the sequences between them (Figures 3c,d, and 5).

Based on the observed products, we hypothesized that the HeLa cells were deferring to a 5' flap cleavage of the nonallelic duplex intermediate (Figures 2f and 4) rather than the typical 3' flap cleavage (Figure 2d). To test this hypothesis we carried out western blots for the ERCC1 protein that is part of the ERCC1/XPF 3' flap endonuclease complex. We chose ERCC1 because of

its tendency to vary extensively in cancer cells (Liu et al., 2013; McGurk et al., 2006; Vaezi et al., 2011). We confirmed that our HeLa cells express a lower level of ERCC1 by immunoblotting and had a significant increase in HD-RMD products compared to HEK293 cells (Figure 4b). For confirmation, we transfected an empty vector and the ERCC1 expression vector to the 0% AARP HeLa cells (Figure 4c). We found that expression of ERCC1 caused a 53% increase of Alu/Alu RMDs when compared to the empty vector control (Figure 4c). These results indicate that low ERCC1 expression in these cells gives rise to this unique breakpoint junction that does not contain an Alu (Figure 2f).

To further test the model that low ERCC1 expression can give rise to this unique HD-RMD repair, we tested the 0% AARP reporter in ERCC1 KO HEK293, which were confirmed as lacking ERCC1 protein by immunoblotting (Figure 4d). We observed that HEK293 cells predominantly gave rise to HD-RMD when ERCC1 was knocked



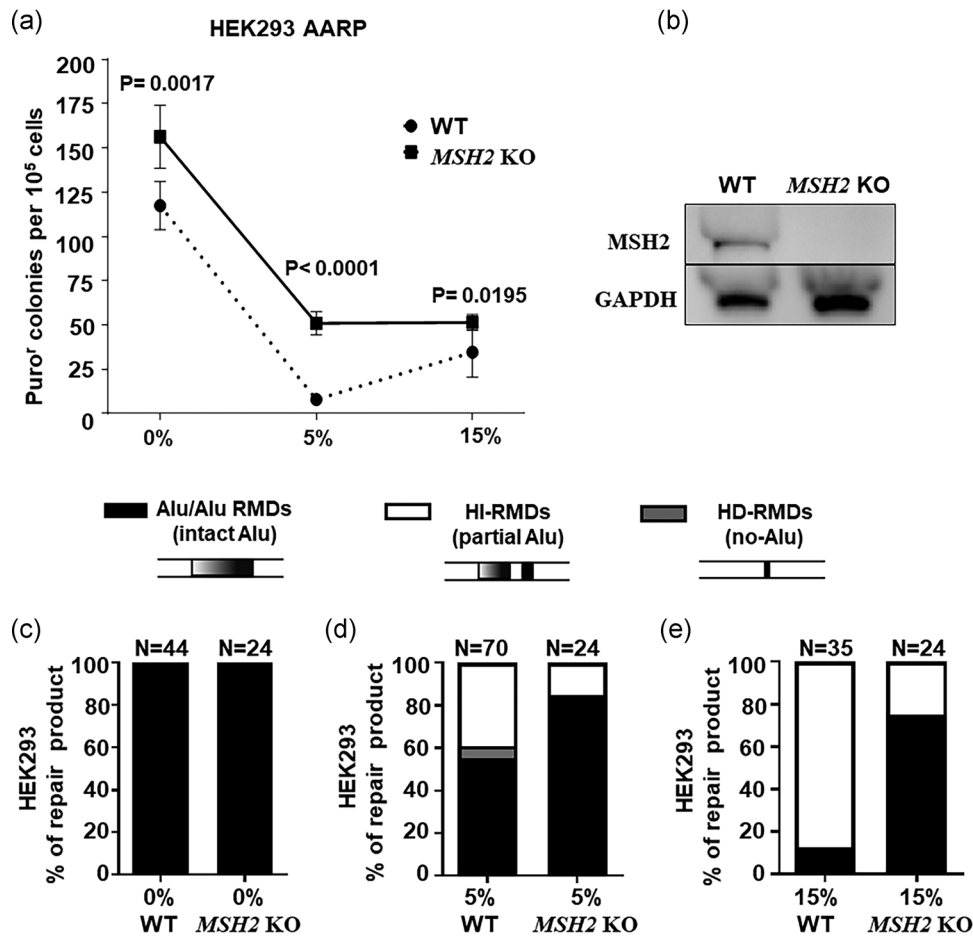


**FIGURE 6** (a) The average number of puro<sup>+</sup> colonies is plotted for AARP WT and MSH2 KO HEK293 cells. Data from at least three independent experiments using at least three independently isolated clones for each AARP cell line are averaged. Error bars denote SE and statistical significance is shown using student t test. Loss of MSH2 increases the rate of Alu/Alu RMDs between divergent repeats. (b) The immunoblot analysis confirming MSH2 KO in HEK293s. These same lanes are repeated in Figure 7a for reference. (c–e) Depicted are the percentages of Alu/Alu RMDs (in black) and HI-RMD (in white) as determined by sequence analysis of DNA repair products from isolated puro<sup>+</sup> colonies in WT and MSH2 KO HEK293 cells. AARP, Alu/Alu recombination puro; KO, knockout; RMD, repeat-mediated deletion

provides evidence that MSH2 and MMR play a role in resolving heteroduplex intermediates that give rise to partial Alus.

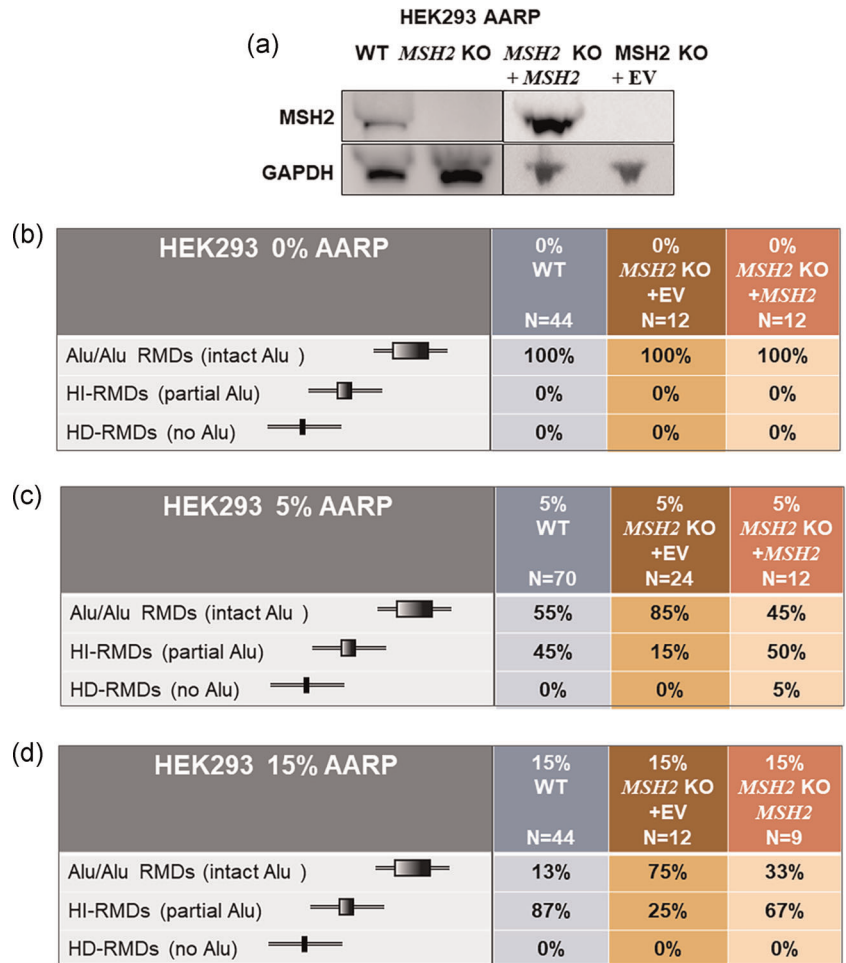
### 3.4 | The influence of RAD52 on Alu-related RMD rate and DSB breakpoint junction

RAD52 is a DNA binding protein that mediates the annealing of DSBs between repeat sequences like nonallelic Alus through SSA-like repair (Figure 1b) (Brouwer et al., 2017; Grimme et al., 2010; Rothenberg et al., 2008). Previously using an siRNA approach, our lab showed that the knockdown of RAD52 resulted in a notable decrease in Alu-related RMDs between homologous Alu elements (Morales, Servant, et al., 2015). To replicate these findings in a more stable approach, we genetically knocked out RAD52 in HEK293 and HeLa cells (confirmed by immunoblot analysis shown in Figure 8b and Figure S6b). Notably, RAD52 KO with 0% AARP resulted in a marked fourfold and twofold decrease in Alu-related RMD rate

compared to WT with 0% AARP in both HEK293 and HeLa cells, respectively (Figure 8a and Figures S5a and S6a). RAD52 KO cells with 5% AARP resulted in a threefold and sevenfold increase in Alu-related RMD rate when compared to WT with 5% AARP in both HEK293 and HeLa cells, respectively (Figure 8a and Figures S5a and S6a). These findings demonstrate that RAD52 mediates the formation of the Alu/Alu heteroduplex for the majority of the events.

Next we analyzed the sequences of breakpoint junctions recovered from the RAD52 KO puro<sup>+</sup> isolated colonies in HEK293 and HeLa cells. Interestingly, RAD52 KO cells with identical Alu sequences resulted in 20% HI-RMD breakpoint junctions compared to 0% HI-RMD breakpoint junctions in HEK293 WT cells (Figure 8c and Figure S7b). HeLa RAD52 KO cells with 0% AARP also gave rise to HD-RMDs (Figures S6c and S8). If RAD52 were the only annealing factor to form SSA-like breakpoint junctions, we would have expected the majority of breakpoint junctions to be resolved with NHEJ. The 5% and 15% mismatched constructs had no significant changes in the apparent resolution of the

**FIGURE 7** (a) The immunoblot analysis confirming MSH2 expression in WT, *MSH2* KO, *MSH2* KO +EV, and *MSH2* complementation vector in HEK293s. The WT and *MSH2* KO lanes are included for reference from Figure 6b. (b–d) Tables summarizing the percentage of Alu/Alu RMDs, HI-RMDs, and HD-RMDs for the WT, *MSH2* KO +EV, and *MSH2* complementation vector in HEK293 cells isolated from puro<sup>r</sup> colonies in the different AARP constructs. KO, knockout; RMD, repeat-mediated deletion



heteroduplexes, in WT and *RAD52* KO in HEK293 or HeLa (Figure 8d,e and Figure S6d,e), despite apparently large differences in heteroduplex formation. *RAD52* complemented RMD breakpoint junctions were similar to WT in HEK293 and HeLa cells (Figures S7 and S8).

### 3.5 | Changes in the Alu/Alu RMD (intact Alu) breakpoint junctions in AARP HEK293 and HeLa *RAD52* and *MSH2* KO cells

It has been shown that Alu/Alu RMD junctions preferentially recombine in the first 100 bps of the Alu element in disease-causing and evolutionary deletions (Bondurand et al., 2012; Kataoka et al., 2013; Kolomietz et al., 2002; Morales et al., 2015; Nozu et al., 2014; Rüdiger et al., 1995; Sen et al., 2006; Wada et al., 2014). In 2015, we also observed the same pattern of recombination in our AARP recombination system using HEK293 WT cells (Figure S9b) (Morales et al., 2015). We further established this recombination pattern in HeLa cells (Figure S9a). To determine if Alu/Alu RMD junctions similarly cluster to a particular region of the participating diverged Alu elements when DNA repair processes are altered, we mapped the recombination junctions of *MSH2* and *RAD52* KO HEK293 and HeLa

cells. In both *MSH2* KO cell lines, we observed a statistically significant increase in the number of recombination junctions occurring within the first 100 bps of the Alu elements when compared to the remaining portions of the Alu (Figure 9b). In both *RAD52* KO cell lines, we observed for the first time a statistically significant increase in the number of recombination junctions occurring within the last 100 bps of the Alu elements when compared to the remaining portions of the Alu (Figure 9c). These findings imply that *RAD52* plays a role in the typical pattern of Alu recombination junctions.

## 4 | DISCUSSION

Alu elements represent the highest copy number of repetitive DNA sequences interspersed throughout the human genome (Lander et al., 2001). Thus, Alu elements provide one of the most active sources of nonallelic homologous sequences that can lead to recombination and related forms of RMDs. For Alu elements to contribute to RMDs, they must first be brought together, either as exposed single-strands following excision at a DSB (Figure 1a) or through a strand-invasion of another nonallelic Alu (Figure 1b) (McVean et al., 2012; Morales et al., 2015; Song et al., 2018). In either case, the nonallelic Alu elements form a heteroduplex. This

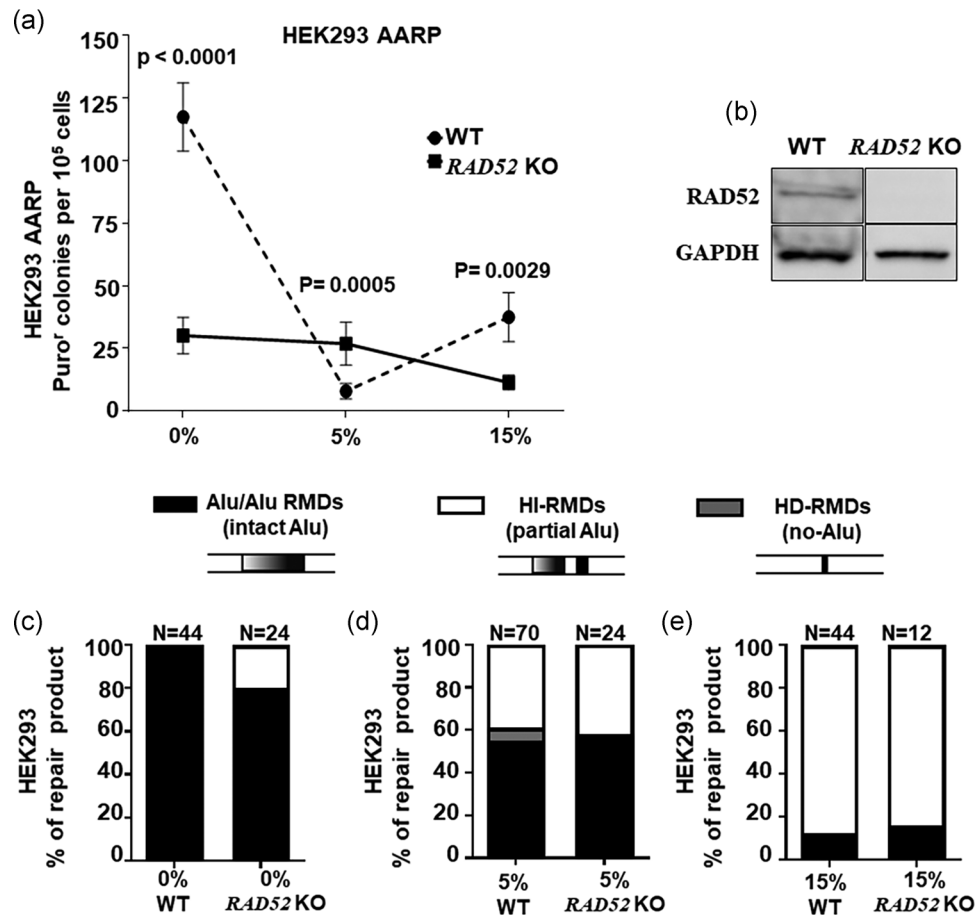


**FIGURE 8** (a) The average number of puro<sup>r</sup> colonies is plotted for AARP WT and RAD52 KO HEK293 cells. Data from at least three independent experiments using at least three independently isolated clones for each AARP cell line are averaged. Error bars denote SE and statistical significance is shown using student *t* test. (b) The immunoblot analysis confirming RAD52 KO in HEK293 cells. The two lanes shown are from different locations that were not adjacent within the same blot and they are also provided for reference in Figure S7a. (c–e) Depicted are the percentages of Alu/Alu RMDs (in black) and HI-RMD (in white) as determined by sequence analysis of DNA repair products from isolated puro<sup>r</sup> colonies in WT and RAD52 KO HEK293 cells. AARP, Alu/Alu recombination puro; KO, knockout; RMD, repeat-mediated deletion

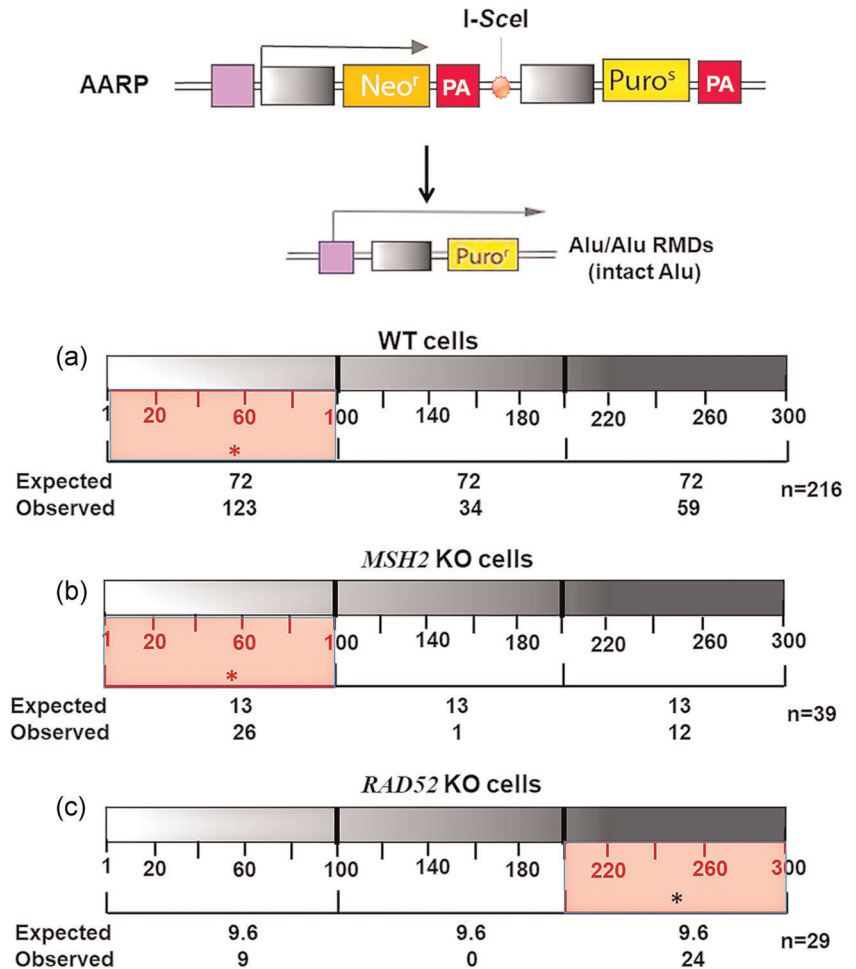
Alu/Alu heteroduplex can vary from almost perfect homology to as much as 30% divergence depending on the evolutionary age of the Alu elements (Batzer & Deininger, 2002). Depending on homology, various DNA repair pathways (MMR, NER) compete with one another to resolve Alu/Alu heteroduplexes (Morales et al., 2015).

The formation of the Alu/Alu heteroduplexes is dependent on either 5' excision of the DNA strand at both ends of a DSB or exposure of a single-ended break by replication up to a single-strand nick (Figure 1b). It is thought that RAD52 is a critical partner in assembling the Alu/Alu heteroduplex if both Alu elements are exposed by excision (Rothenberg et al., 2008). RAD51 is critical for invasion by single-ended breaks, but RAD52 may also facilitate some of those interactions (Bhowmick et al., 2016; Sotiriou et al., 2016). The measurements in this paper utilize I-Sce1 to generate a DSB and our findings in both HeLa and HEK293 cells suggest that most of the Alu-related RMDs utilize RAD52, as the majority of the colonies are lost when RAD52 is knocked out (Figure 8a and Figures S5a and S6a). Our studies are carried out with a 1.1 kb spacing between the Alu

elements (see Figure 2), which is a typical spacing in the genome. However, it is also likely that the location of the DSB relative to the Alu elements and the spacing of the elements will affect factors such as resection and the details of which mechanisms (i.e., SSA vs. BIR) are utilized to bring the Alu elements together (Mendez-Dorantes et al., 2018; Hu et al., 2019).

Once the Alu/Alu heteroduplex forms, we propose that there are different DNA repair processes that compete to resolve it. The first process could be heteroduplex rejection mediated through MSH2 and helicases. ERCC1/XPF could also cleave the 3' tails necessary for resolution (Figure 2d). Then MMR with nucleases could cleave at the mismatches to create new DNA ends, which are then repaired by alt-NHEJ resulting in HI-RMDs (Figure 2e). Finally, when levels of ERCC1/XPF are reduced, other nucleases could cleave at the 5' flaps of the Alu/Alu heteroduplex, which are repaired by alt-NHEJ to form HD-RMDs (Figure 2f). The resulting repairs reflect which pathways are more efficient for Alu/Alu heteroduplex resolution in that particular cell DNA repair background.

**FIGURE 9** (a–c) The distribution of Alu/Alu RMD junctions in diverged AARPs (5% and 15%) in combined WT, *MSH2* KO, and *RAD52* KO HEK293 and HeLa cells. The Alu/Alu RMD product is divided into three equal segments (100 bps), with each contain the same extent of sequence divergence. The number of Alu/Alu RMDs expected and observed in each 100 bp interval is shown. An asterisk (\*) represents  $p < .05$  significance as determined by  $\chi^2$  test for observed versus expected. AARP, Alu/Alu recombination puro; KO, knockout; RMD, repeat-mediated deletion



We found that the HeLa cells routinely used in our laboratory have only low levels of ERCC1 expression, resulting in the apparent use of a 5' flap endonuclease on the perfectly matched heteroduplex (Figure 4b). These results in removal of both Alu elements and the DNA between them when the new ends generated by the 5' flap endonuclease are cleaved (Figures 2f and 4). Here we show for the first time HD-RMD (alt-NHEJ) that gives rise to a unique breakpoint junction. Expressing increased levels of ERCC1 in these HeLa cells resulted in a return to the more classic SSA-like resolution using the 3' endonuclease (Figure 4c). When the heteroduplex has mismatches, endonuclease cleavage at the mismatches seems to be prioritized over the 5' endonuclease cleavage in HeLa cells, producing the HI-RMDs product (Figure 3c).

Other cells with typical cancer-related mismatch-repair deficiencies, like *MSH2* and *MLH1*, will also differ in how they resolve the nonallelic, Alu/Alu heteroduplexes. Because of the loss of heteroduplex rejection, both HEK293 and HeLa cells showed a significant increase in Alu-related RMDs when *MSH2* was knocked out. Not surprisingly, these influences were proportionately greater when mismatches were present between the Alu elements (Figure 6b,c). Studies in RMD events in *MSH2* KO mouse embryonic stem cells had previously shown similar stimulation of RMDs (Mendez-Dorantes et al., 2018; 2020) suggesting that Alu elements are likely to play a

bigger role in resolution of DSBs in this specific cell background. *MLH1* deficiency, which does not effect heteroduplex rejection, will have a much smaller, deleterious role with decreased formation of Alu-related RMDs (Morales et al., 2015).

Our data demonstrate that the level and types of DNA rearrangements to which Alu elements contribute should be expected to vary tremendously from one cancer to another depending on the relative activity of many DNA repair factors. The density of Alu elements and the level of mismatch between them will influence types of Alu-related RMDs described in this study in different regions of the genome. Many hotspots for Alu/Alu recombination have been reported from genome analysis. Here we add to the Alu-related RMD studies using a reporter gene system that allows measurement of rate differences to detect less precise processes, such as HI-RMDs and HD-RMDs. These processes with unique breakpoint junctions are integral in understanding the contribution of Alu elements to mutagenic deletions and rearrangements that could lead to disease.

#### ACKNOWLEDGMENTS

The authors would like to thank Dr. Astrid Engel and other members of the Consortium of Mobile Elements for invaluable advice and critical discussion. The authors thank Mary Price and the Louisiana

Cancer Research Consortium FACS Core for assistance with FACS analysis. The authors wish to sincerely thank Karen Jones, Alton-nesha Darby, Jerrica Harris, and Brittany Russell who helped with tissue cell culture and genomic extractions. Funding was provided by NIH grant R01 GM121812 (to PD) and grant RL5 GM118966 (to JW).

### CONFLICT OF INTERESTS

The authors declare that there are no conflict of interests.

### AUTHOR CONTRIBUTIONS

**Prescott Deininger, Maria E. Morales, and Travis White:** conceived and designed experiments. **Maria E. Morales, Tiffany Kaul, Chelsea Everett, and JaNiece Walker:** performed experiments. **Prescott Deininger, Maria E. Morales, and Tiffany Kaul:** analyzed the data and wrote the paper.

### DATA AVAILABILITY STATEMENT

All data, including plasmids, cell lines and DNA sequences reported in this study are freely available through a request to the corresponding author (Prescott Deininger).

### ORCID

Prescott Deininger  <http://orcid.org/0000-0002-1067-3028>

### REFERENCES

- Al-Minawi, A. Z., Saleh-Gohari, N., & Helleday, T. (2008). The ERCC1/XPF endonuclease is required for efficient single-strand annealing and gene conversion in mammalian cells. *Nucleic Acids Research*, 36(1), 1–9. <https://doi.org/10.1093/nar/gkm888>
- Batzer, M. A., & Deininger, P. L. (2002). Alu repeats and human genomic diversity. *Nature Reviews Genetics*, 3(5), 370–379. <https://doi.org/10.1038/nrg798>
- Belancio, V. P., Roy-Engel, A. M., & Deininger, P. L. (2010). All y'all need to know 'bout retroelements in cancer. *Seminars in Cancer Biology*, 20(4), 200–210. <https://doi.org/10.1016/j.semcancer.2010.06.001>
- Bhargava, R., Onyango, D. O., & Stark, J. M. (2016). Regulation of single-strand annealing and its role in genome maintenance. *Trends in genetics: TIG*, 32(9), 566–575. <https://doi.org/10.1016/j.tig.2016.06.007>
- Bhowmick, R., Minocherhomji, S., & Hickson, I. D. (2016). RAD52 facilitates mitotic DNA synthesis following replication stress. *Molecular Cell*, 64(6), 1117–1126. <https://doi.org/10.1016/j.molcel.2016.10.037>
- Bondurand, N., Fouquet, V., Baral, V., Lecerf, L., Loundon, N., Goossens, M., Duriez, B., Labrune, P., & Pingault, V. (2012). Alu-mediated deletion of SOX10 regulatory elements in Waardenburg syndrome type 4. *European Journal Of Human Genetics: EJHG*, 20(9), 990–994. <https://doi.org/10.1038/ejhg.2012.29>
- Brouwer, I., Zhang, H., Candelli, A., Normanno, D., Peterman, E. J. G., Wuite, G. J. L., & Modesti, M. (2017). Human RAD52 captures and holds DNA strands, increases DNA flexibility, and prevents melting of duplex DNA: Implications for DNA recombination. *Cell Reports*, 18(12), 2845–2853. <https://doi.org/10.1016/j.celrep.2017.02.068>
- Callinan, P. A., Wang, J., Herke, S. W., Garber, R. K., Liang, P., & Batzer, M. A. (2005). Alu retrotransposition-mediated deletion. *Journal of Molecular Biology*, 348(4), 791–800. <https://doi.org/10.1016/j.jmb.2005.02.043>
- Chakraborty, U., & Alani, E. (2016). Understanding how mismatch repair proteins participate in the repair/anti-recombination decision. *FEMS Yeast Research*, 16(6), fow071. <https://doi.org/10.1093/femsyr/fow071>
- Cordaux, R., & Batzer, M. A. (2009). The impact of retrotransposons on human genome evolution. *Nature Reviews Genetics*, 10(10), 691–703. <https://doi.org/10.1038/nrg2640>
- Deininger, P. L., & Batzer, M. A. (1999). Alu repeats and human disease. *Molecular Genetics and Metabolism*, 67(3), 183–193. <https://doi.org/10.1006/mgme.1999.2864>
- Grimme, J. M., Honda, M., Wright, R., Okuno, Y., Rothenberg, E., Mazin, A. V., Ha, T., & Spies, M. (2010). Human Rad52 binds and wraps single-stranded DNA and mediates annealing via two hRad52-ssDNA complexes. *Nucleic Acids Research*, 38(9), 2917–2930. <https://doi.org/10.1093/nar/gkp1249>
- Gu, S., Yuan, B., Campbell, I. M., Beck, C. R., Carvalho, C. M., Nagamani, S. C., Erez, A., Patel, A., Bacino, C. A., Shaw, C. A., Stankiewicz, P., Cheung, S. W., Bi, W., & Lupski, J. R. (2015). Alu-mediated diverse and complex pathogenic copy-number variants within human chromosome 17 at p13.3. *Human Molecular Genetics*, 24(14), 4061–4077. <https://doi.org/10.1093/hmg/ddv146>
- Hedges, D. J., Callinan, P. A., Cordaux, R., Xing, J., Barnes, E., & Batzer, M. A. (2004). Differential alu mobilization and polymorphism among the human and chimpanzee lineages. *Genome Research*, 14(6), 1068–1075. <https://doi.org/10.1101/gr.2530404>
- Hu, Q., Lu, H., Wang, H., Li, S., Truong, L., Li, J., Liu, S., Xiang, R., & Wu, X. (2019). Break-induced replication plays a prominent role in long-range repeat-mediated deletion. *The EMBO Journal*, 38(24), e101751. <https://doi.org/10.15252/embj.2019101751>
- Kass, E. M., & Jasin, M. (2010). Collaboration and competition between DNA double-strand break repair pathways. *FEBS Letters*, 584(17), 3703–3708. <https://doi.org/10.1016/j.febslet.2010.07.057>
- Kataoka, M., Aimi, Y., Yanagisawa, R., Ono, M., Oka, A., Fukuda, K., Yoshino, H., Satoh, T., & Gamou, S. (2013). Alu-mediated nonallelic homologous and nonhomologous recombination in the BMP2 gene in heritable pulmonary arterial hypertension. *Genetics in Medicine*, 15(12), 941–947. <https://doi.org/10.1038/gim.2013.41>
- Kaul, T. K., Morales, M. E., Deininger, P. L. (2017). *L. John Wiley & Sons Repetitive Elements and Human Disorders eLS*.
- Kolomietz, E., Meyn, M. S., Pandita, A., & Squire, J. A. (2002). The role of Alu repeat clusters as mediators of recurrent chromosomal aberrations in tumors. *Genes, Chromosomes and Cancer*, 35(2), 97–112. <https://doi.org/10.1002/gcc.10111>
- Lander, E. S., Linton, L. M., Birren, B., Nusbaum, C., Zody, M. C., Baldwin, J., & The Wellcome, T. (2001). Initial sequencing and analysis of the human genome. *Nature*, 409(6822), 860–921. <https://doi.org/10.1038/35057062>
- Liu, Y.-P., Ling, Y., Qi, Q.-F., Zhang, Y.-P., Zhang, C.-S., Zhu, C.-T., WANG, M. H., & PAN, Y. D. (2013). The effects of ERCC1 expression levels on the chemosensitivity of gastric cancer cells to platinum agents and survival in gastric cancer patients treated with oxaliplatin-based adjuvant chemotherapy. *Oncology Letters*, 5(3), 935–942. <https://doi.org/10.3892/ol.2012.1096>
- Mátés, L., Chuah, M. K. L., Belay, E., Jerchow, B., Manoj, N., Acosta-Sanchez, A., Grzela, D. P., Schmitt, A., Becker, K., Matrai, J., Ma, L., Samara-Kuko, E., Gysemans, C., Pryputniewicz, D., Miskey, C., Fletcher, B., VandenDriessche, T., Ivics, Z., & Izsvák, Z. (2009). Molecular evolution of a novel hyperactive sleeping beauty transposase enables robust stable gene transfer in vertebrates. *Nature Genetics*, 41(6), 753–761. <https://doi.org/10.1038/ng.343>
- McGurk, C. J., Cummings, M., Köberle, B., Hartley, J. A., Oliver, R. T., & Masters, J. R. (2006). Regulation of DNA repair gene expression in human cancer cell lines. *Journal of Cellular Biochemistry*, 97(5), 1121–1136. <https://doi.org/10.1002/jcb.20711>
- McVean, G. A., Altshuler, D. M., Durbin, R. M., Abecasis, G. R., Bentley, D. R., Chakravarti, A., & University of, G. (2012).

- An integrated map of genetic variation from 1,092 human genomes. *Nature*, 491(7422), 56–65. <https://doi.org/10.1038/nature11632>
- Mendez-Dorantes, C., Bhargava, R., & Stark, J. M. (2018). Repeat-mediated deletions can be induced by a chromosomal break far from a repeat, but multiple pathways suppress such rearrangements. *Genes & Development*, 32(7-8), 524–536. <https://doi.org/10.1101/gad.311084.117>
- Mendez-Dorantes, C., Tsai, L. J., Jahanshir, E., Lopezcolorado, F. W., & Stark, J. M. (2020). BLM has contrary effects on repeat-mediated deletions, based on the Distance of DNA DSBs to a repeat and repeat divergence. *Cell Reports*, 30(5), 1342–1357. <https://doi.org/10.1016/j.celrep.2020.01.001>
- Morales, M. E., Servant, G., Ade, C. M., & Deininger, P. (2015). Alu-Alu recombinations in genetic diseases. *Human Retrotransposons in Health and Disease* (pp. 239–257). Springer Publishing.
- Morales, M. E., White, T. B., Strevva, V. A., DeFreece, C. B., Hedges, D. J., & Deininger, P. L. (2015). The contribution of Alu elements to mutagenic DNA double-strand break repair. *PLoS Genetics*, 11(3), e1005016. <https://doi.org/10.1371/journal.pgen.1005016>
- Nozu, K., Iijima, K., Ohtsuka, Y., Fu, X. J., Kaito, H., Nakanishi, K., & Vorechovsky, I. (2014). Alport syndrome caused by a COL4A5 deletion and exonization of an adjacent AluY. *Molecular Genetics & Genomic Medicine*, 2(5), 451–453. <https://doi.org/10.1002/mgg3.89>
- Pavlicek, A., Noskov, V. N., Kouprina, N., Barrett, J. C., Jurka, J., & Larionov, V. (2004). Evolution of the tumor suppressor BRCA1 locus in primates: Implications for cancer predisposition. *Human Molecular Genetics*, 13(22), 2737–2751. <https://doi.org/10.1093/hmg/ddh301>
- Rothenberg, E., Grimme, J. M., Spies, M., & Ha, T. (2008). Human Rad52-mediated homology search and annealing occurs by continuous interactions between overlapping nucleoprotein complexes. *Proceedings of the National Academy of Sciences*, 105(51), 20274–20279. <https://doi.org/10.1073/pnas.0810317106>
- Rüdiger, N. S., Gregersen, N., & Kielland-Brandt, M. C. (1995). One short well conserved region of Alu-sequences is involved in human gene rearrangements and has homology with prokaryotic chi. *Nucleic Acids Research*, 23(2), 256–260. <https://doi.org/10.1093/nar/23.2.256>
- Sanger, F., Nicklen, S., & Coulson, A. R. (1977). DNA sequencing with chain-terminating inhibitors. *Proceedings of the National Academy of Sciences of the United States of America*, 74(12), 5463–5467. <https://doi.org/10.1073/pnas.74.12.5463>
- Sen, S. K., Han, K., Wang, J., Lee, J., Wang, H., Callinan, P. A., Dyer, M., Cordaux, R., Liang, P., & Batzer, M. A. (2006). Human genomic deletions mediated by recombination between Alu elements. *American Journal of Human Genetics*, 79(1), 41–53. <https://doi.org/10.1086/504600>
- Servant, G., Strevva, V. A., Derbes, R. S., Wijetunge, M. I., Neeland, M., White, T. B., Belancio, V. P., Roy-Engel, A. M., & Deininger, P. L. (2017). The nucleotide excision repair pathway limits L1 retrotransposition. *Genetics*, 205(1), 139–153. <https://doi.org/10.1534/genetics.116.188680>
- Song, X., Beck, C. R., Du, R., Campbell, I. M., Coban-Akdemir, Z., Gu, S., Breman, A. M., Stankiewicz, P., Ira, G., Shaw, C. A., & Lupski, J. R. (2018). Predicting human genes susceptible to genomic instability associated with Alu/Alu-mediated rearrangements. *Genome Research*, 28(8), 1228–1242. <https://doi.org/10.1101/gr.229401.117>
- Sotiriou, S. K., Kamileri, I., Lugli, N., Evangelou, K., Da-Ré, C., Huber, F., Padayachy, L., Tardy, S., Nicati, N. L., Barriot, S., Ochs, F., Lukas, C., Lukas, J., Gorgoulis, V. G., Scapozza, L., & Halazonetis, T. D. (2016). Mammalian RAD52 functions in break-induced replication repair of collapsed DNA replication forks. *Molecular Cell*, 64(6), 1127–1134. <https://doi.org/10.1016/j.molcel.2016.10.038>
- Sugawara, N., Goldfarb, T., Studamire, B., Alani, E., & Haber, J. E. (2004). Heteroduplex rejection during single-strand annealing requires Sgs1 helicase and mismatch repair proteins Msh2 and Msh6 but not Pms1. *Proceedings of the National Academy of Sciences of the United States of America*, 101(25), 9315–9320. <https://doi.org/10.1073/pnas.0305749101>
- Symington, L. S., & Gautier, J. (2011). Double-strand break end resection and repair pathway choice. *Annual Review of Genetics*, 45(1), 247–271. <https://doi.org/10.1146/annurev-genet-110410-132435>
- Vaezi, A., Feldman, C. H., & Niedernhofer, L. J. (2011). ERCC1 and XRCC1 as biomarkers for lung and head and neck cancer. *Pharmacogenomics and Personalized Medicine*, 4, 47–63. <https://doi.org/10.2147/PGPM.S20317>
- Wada, T., Matsuda, Y., Muraoka, M., Toma, T., Takehara, K., Fujimoto, M., & Yachie, A. (2014). Alu-mediated large deletion of the CDSN gene as a cause of peeling skin disease. *Clinical Genetics*, 86(4), 383–386. <https://doi.org/10.1111/cge.12294>
- White, T. B., Morales, M. E., & Deininger, P. L. (2015). Alu elements and DNA double-strand break repair. *Mobile Genetic Elements*, 5(6), 81–85. <https://doi.org/10.1080/2159256X.2015.1093067>
- Xing, J., Witherspoon, D. J., Ray, D. A., Batzer, M. A., & Jorde, L. B. (2007). Mobile DNA elements in primate and human evolution. *American Journal of Physical Anthropology*, 134(S45), 2–19. <https://doi.org/10.1002/ajpa.20722>

## SUPPORTING INFORMATION

Additional Supporting Information may be found online in the supporting information tab for this article.

**How to cite this article:** Morales, M. E., Kaul, T., Walker, J., Everett, C., White, T., & Deininger, P. (2021). Altered DNA repair creates novel Alu/Alu repeat-mediated deletions. *Human Mutation*, 42, 600–613. <https://doi.org/10.1002/humu.24193>